JOURNAL OF MATERIALS SCIENCE 33 (1998) 2005–2012

Effects of the process conditions during dry-defibration on the properties of cellulosic networks

C. ASKLING, L. WÅGBERG
SCA Research AB, Box 3054, S-850 03 Sundsvall, Sweden
M. RIGDAHL
Swedish Pulp and Paper Research Institute (STFI), Box 5604, S-114 86, Stockholm, Sweden

The influence of structural changes caused by dry-defibration of the pulp on the mechanical properties of dry-formed cellulosic networks has been investigated. The effects of fibre length, fibre curl and content of fine material on these properties are discussed. The fluff pulps used were one CTMP-grade and two kraft pulps. The primary parameters used to describe the networks were the storage modulus, $\mathbf{G}'_0$ (measured at low strain amplitudes), and the critical strain, γ_c (at which the network yields), obtained from dynamic-mechanical measurements, and the maximum force, F_{max}, sustained by the network and the maximum strain, γ_{max} (at F_{max}), measured with a specially constructed shear tester. It was noted that the storage shear modulus, $\mathbf{G}'_0$, and maximum force, F_{max}, were affected in the same manner by the defibration conditions. To improve the deformability of the cellulosic network before rupturing, the ideal dry-defibration process should provide a greater number of free fibres per unit volume without producing fine material, at the same time as the curl index of the fibres should increase. Long and curled fibres are thus to be preferred. © *1998 Chapman & Hall*

1. Introduction

The core in hygiene products such as disposable nappies (diapers) is today based on a cellulosic network made from fluff pulp. In order to give a good performance of the product, the core must have a sufficient liquid absorption capacity and also good mechanical stability, i.e. the network must be able to withstand deformation without rupture. To achieve this, the fluff pulp must be well-defibrated, i.e. must consist of free fibres with few inhomogeneities such as knots, flocs and damaged fibres.

The dry-defibration of fluff pulp is hence an important process step in the manufacture of disposable nappies. The defibration is conducted either in hammer mills or in refiners. Despite the common use of hammer mills, the most commonly used defibration equipment today, there is still only a limited understanding of the relation between the defibration conditions and the mechanical properties of the final dry-formed fibre networks. The importance of the defibration process for pulp properties such as absorption time, absorption capacity and knot content has, however, been investigated [1–2].

There may be several reasons for this lack of knowledge, but one important factor is the lack of suitable test equipment for characterizing the mechanical properties of these dry-formed networks. The possibility of using equipment for the evaluation of viscoelastic properties of low-density dry-formed fibre networks was, however, discussed in a previous investigation [3]. This work showed that rheological measurements can provide relevant information regarding the relationship between fibre properties, the structure of a dry-formed fibre network and the mechanical properties of the network. Therefore, it was considered both relevant and interesting to apply this technique to characterize the influence of the defibration process on the properties of such dry-formed networks.

The mechanical properties were also evaluated by determining the network strength, a common measure for characterizing dry-formed fibre networks, using the PFI-network strength tester [4]. A specially constructed equipment for mechanical testing in the shear mode was also used to characterize the networks.

The purpose of the present work was therefore to describe how the mechanical properties of a dry-formed cellulosic network are influenced by the structural changes which can be related to the dry-defibration process. The influence of fibre length, fibre curl and content of fine material on the mechanical properties are also considered. Correlations between the results of the different measuring techniques are also discussed.

This investigation is divided into three parts. The first deals with the influence of the defibration energy

applied to the fibres in the defibration process on the mechanical behaviour and the second part with the mechanical properties of networks made from different fractions of a well-defibrated pulp. In the last part, different fluff pulps with different fibre geometries are compared with regard to their influence on the mechanical properties of the fibre network.

2. Experimental procedure

2.1. Materials

The fibres used in the first and second parts were flash-dried softwood (Norway spruce) fibres from a Chemo Thermo Mechanical Pulp, CTMP (SCA Graphic, Sundsvall AB, Sweden) delivered in bale form. The fibres used in the defibration investigation were defibrated in a hammer mill, manufactured by ROTOM AB, Sundsvall, Sweden, fitted with a sieving plate with holes of 15 mm diameter. The diameter of the rotor was 0.34 m and the number of beater bars was 36/360°. A schematic drawing of the rotor is presented in Fig. 1. The feeding rate of the pulp was 200 g min^{-1}. Five different rotor speeds were used: 500, 1500, 2500, 3500 and 4500 r.p.m.

The defibrated samples were each divided into two parts. One part was kept unfractionated and the other was fractionated in order to remove the fine material. The pulp was fractionated in the dry state with a laboratory sieving machine, type plane, from Retsch (Germany). The mesh width of the sieve used was 300 μm. The oscillation frequency was 4 Hz and the swing diameter 30 mm. 10 g pulp was fractionated for 20 min and the long-fibre fractions were collected and used in the experiments. Details of the different defibrated samples are given in Table I. The fibre length was in all cases determined with a Kajaani FS-100 (Kajaani OY, Finland) and the curl index was defined as the ratio of the fibre length, L_0, to the longest linear distance in the fibre, L, minus 1 ($C = L_0/L - 1$). There was only a minor increase in the curl index as a result of the defibration, but the increase was nevertheless, significant. The curl index for the sample defibrated at 3500 r.p.m. differed from the others, as is evident in Table I. The reason is not clear, but a difference was also apparent in the mechanical properties.

The fibres used in part two, i.e. the fractionation investigation, were defibrated in the same hammer mill. The rotor speed was 2600 r.p.m. and the diameter of the holes in the sieving plate was 15 mm. The operating conditions for the mill were chosen to give the pulp a maximum network strength as measured according to the PFI-method [4]. After defibration to the maximum network strength, the pulp was fractionated using the Retsch sieving machine. Four sieves with mesh numbers 120, 50, 35 and 16 were used. The corresponding widths of the meshes were 125, 300, 500 and 1800 μm. Typically, 10 g pulp was fractionated for 10 min and the vibration frequency and amplitude were the same as before. Details of the different fibre fractions are given in Table II. The fine material <120 mesh and knots and flocs >16 mesh were discarded and not used when forming the fibre networks.

The fluff pulps used in the third part of this study were one CTMP-grade, the same as that in the first and second parts, and two kraft pulps. One kraft pulp was made of Scandinavian softwood (Vigorfluff EN, Korsnäs AB, Sweden) and the other of Southern pine (NB 416, Weyerhaeuser, USA). The pulps were defibrated in the hammer mill but not fractionated. The rotor speeds were 2600, 3200 and 3000 r.p.m. for CTMP, Scandinavian kraft and Southern pine kraft, respectively. The diameter of the holes in the sieving plate was 15 mm. The fibre morphology of the three pulps differed from each other, see. Fig. 2. The CTMP fibres were thick and straight and almost all had a circular cross-section. The fibres of the two kraft pulps were thin and ribbon-like. The fibre lengths were 2.41, 2.17 and 2.68 mm $\pm$ 0.03 mm and the fibre thicknesses were 38.6, 25.9 and 28.5 μm $\pm$ 0.4 μm for CTMP, Scandinavian kraft and Southern pine kraft, respectively. The fibre thickness was determined with the STFI-Fibermaster [5].

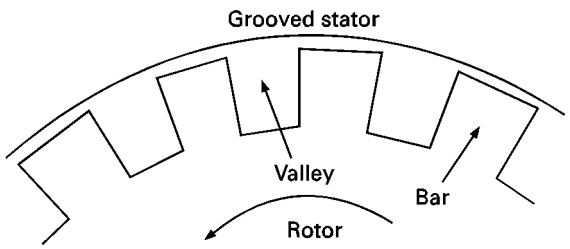

Figure 1 Schematic drawing of the rotor in the hammer mill.

2.2. Sample preparation

After defibration, and in some cases after fractionation, fibre networks were formed with a test specimen former schematically shown in Fig. 3 and further described in SCAN – C33:80. The former was

TABLE I Details of the different defibrated samples

Rotor speed (r.p.m.)	Fibre length, weight average (mm $\pm$ 0.03 mm)	Curl index	Fine material fraction (%)
500	2.43	0.21	26
1500	2.26	0.25	31
2500	2.36	0.25	39
3500	2.21	0.21	48
4500	1.87	0.25/0.26	57

TABLE II Details of the fibre fractions

Fraction	Fibre length weight average (mm $\pm$ 0.03 mm)	Part of pulp (%)
>16 mesh	—	23
16–35 mesh	3.22	36
35–50 mesh	2.45	20
50–120 mesh	1.53	14
<120 mesh	—	7

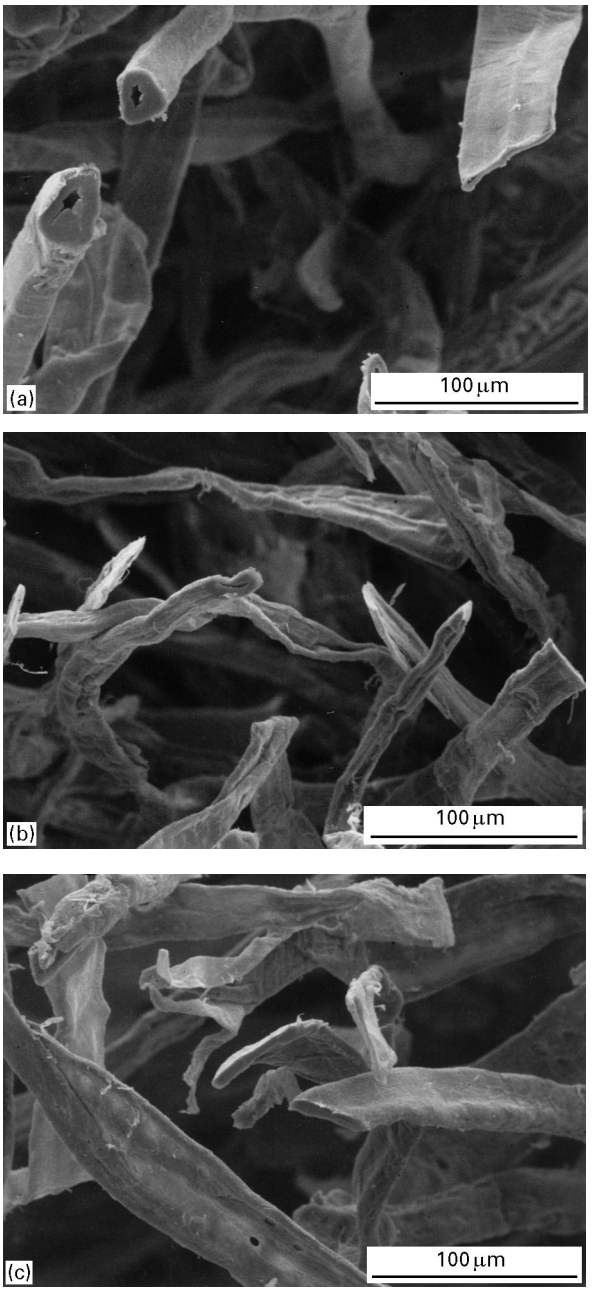

Figure 2 Scanning electron micrographs of the fluff pulps: (a) CTMP, (b) Scandinavian kraft-Vigorfluff, and (c) Southern pine kraft-NB 416.

equipped with special tubes which formed test specimens suitable for the different mechanical evaluations. The density of the networks was 100 kg m^{-3} and the grammage 500 g m^{-2} in all the experiments.

2.3. Dynamic-mechanical analysis

The dynamic-mechanical measurements were performed with a Bohlin VOR Rheometer (Bohlin Reologi AB, Sweden) at room temperature. The samples were conditioned at 23 °C and 50% relative humidity (RH) before the measurements were peformed. The test specimens, with a diameter of 30 mm, were inserted between serrated plates and subjected to torsion around the cylinder axis. The frequency was 1 Hz and the applied shear strain amplitude was varied between 0.2 and 20 mrad.

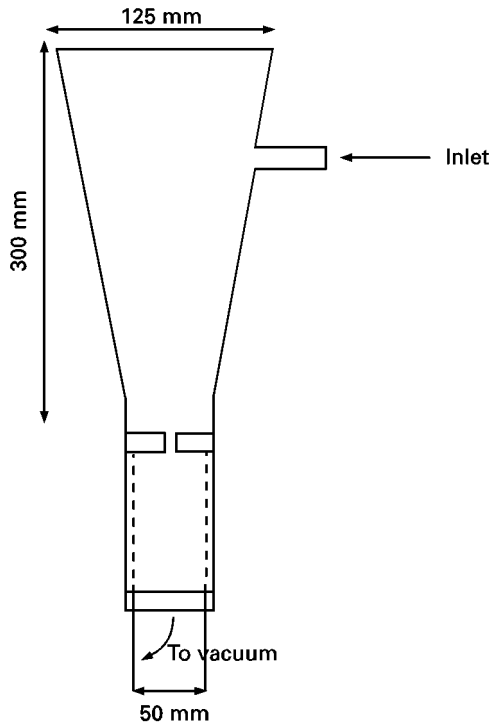

Figure 3 Schematic drawing of the test specimen former.

When performing the dynamic-mechanical analysis, the storage shear modulus, G', was evaluated as a function of the shear strain amplitude of the applied sinusoidal deformation, Fig. 4.

In general, the storage modulus decreased as the strain amplitude increased. In fact, G' was fairly constant for small strains and the value of the storage modulus at a strain amplitude of 0.0007 was taken as G'_0, the shear modulus of the undisturbed network, cf. Fig. 4. The intersection of the two straight lines depicted in Fig. 4 gives a critical strain, γ_c. Somewhat simplified, it may be said that for strains larger than γ_c, the network gradually breaks down. Another way of expressing this, is that the network is regarded as being approximately linearly viscoelastic at strains lower than γ_c.

In addition to the critical strain, γ_c, the ultimate properties of the network can be described by the stored elastic energy at γ_c (W_{el}) given by

$$W_{el} = \frac{1}{2} G'_0 (\gamma_c)^2 \quad (1)$$

2.4. Strength properties of the network

Because measurements with the Bohlin VOR provide, in a sense, information on the micromechanics of the networks, it was, as a complement, considered vital to evaluate the macroscopic network properties of the same networks in order to relate to the end-use performance of the networks. The strength properties were then evaluated by measuring the maximum force which the network could withstand and the work of deformation to break in the shear mode with a specially designed equipment. The following standard procedure was used for the shear testing of the dry-formed networks. Test specimens, with

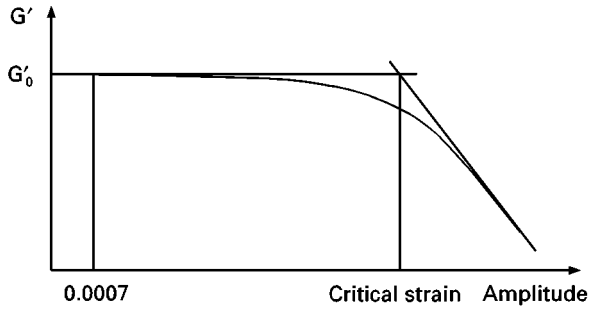

Figure 4 Schematic representation of the relation between G' and the shear strain amplitude.

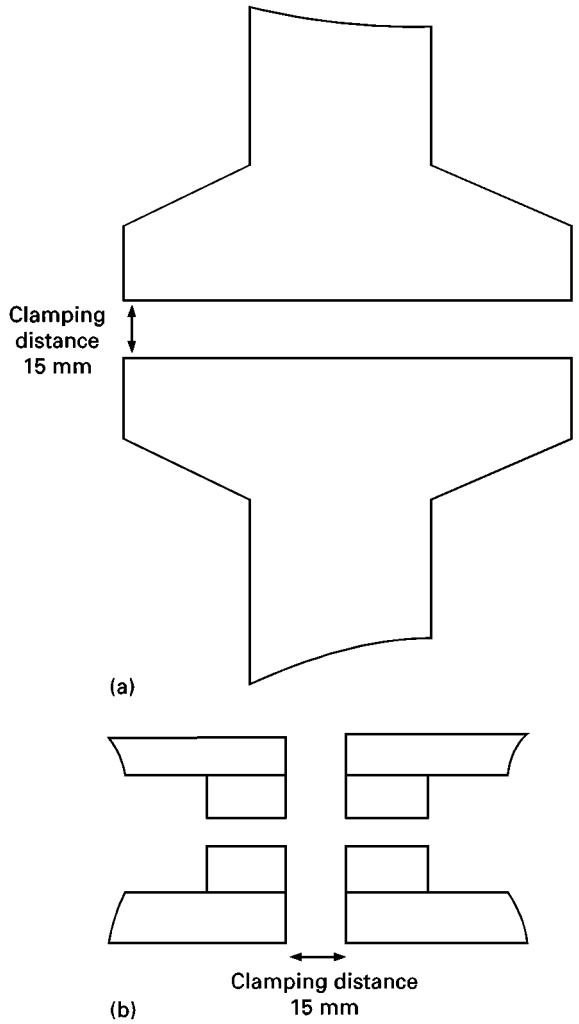

Figure 5 Schematic drawing of the clamps of the shear tester: (a) viewed from above, (b) side view.

dimensions of 30 mm × 50 mm, were mounted with a clamping distance of 15 mm, schematically shown in Fig. 5, and sheared at a deformation rate of 1 mm s^{-1}. During the deformation, the force was continuously recorded by a load cell that was mounted on one of the clamps. In order to be able to record the small forces involved, special load cells, Bofors U2D1 (Bofors AB, Sweden), were used. The force was plotted as a function of the deformation, as shown schematically in Fig. 6, and the following entities were defined: F_{max} is the maximum force recorded, F_{break} is 50% of maximum force (after the maximum is passed), γ_{max} is

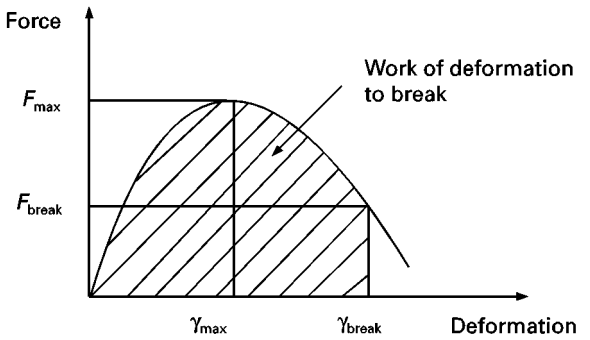

Figure 6 Schematic diagram showing the relation between the measured force and the shear deformation when using the specially designed mechanical tester.

(deformation/clamping distance) at maximum force, and γ_{break} the (deformation/clamping distance) at break.

Prior to the measurements, the samples were conditioned overnight at 23 °C and 50% RH and the tests were then conducted under the same conditions. The mechanical properties of the networks were further characterized by determining the network strength using the PFI-network strength tester [4].

3. Results and comments

3.1. Influence of the defibration energy on G'_0 and γ_c

Fig. 7 shows the storage shear modulus G'_0 of the CTMP networks as a function of the rotor speed of the hammer mill during the defibration. The higher the rotor speed, the greater is the defibration energy applied to the fibres. Results for both fractionated and unfractionated pulps are shown in the figure. The storage shear modulus first increased with increasing rotor speed, passed through a maximum and then decreased. The decrease was more pronounced in the case of the unfractionated pulp, i.e. when the fine material was still present.

The influence of the rotor speed on the critical strain, γ_c, is shown in Fig. 8. Increasing rotor speed resulted in a higher critical strain value for the CTMP networks. The increase was more pronounced when the networks were based on fractionated pulp.

When the energy input to the pulp during defibration is increased, several events may be initiated. First, more fibres are liberated and the number of free single fibres per unit volume thus increases. At the same time, the fibres may become wrinkled or even cut by the bars in the rotor. However, considering the distance between the stator and the rotor, 3 mm in Fig. 1, it is probable that fibre bundles are destroyed before any single fibre is cut. With this in mind, it may be suggested that the initial increase in G'_0 when the rotor speed is raised is due to an increase in the volume concentration of free fibres. This increase will lead to a shorter free segment length between two fibre crossings in the network, and hence to a higher G'_0 (cf. [3]).

The decrease in the storage modulus at higher rotor speeds can be due both to a creation of ineffective fine material (which cannot transfer stress throughout the

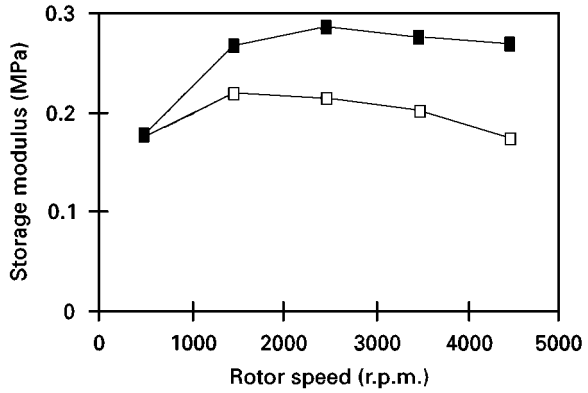

Figure 7 The storage shear modulus, G'_0, as a function of rotor speed of the hammer mill for networks based on (□) unfractionated or (■) fractionated CTMP.

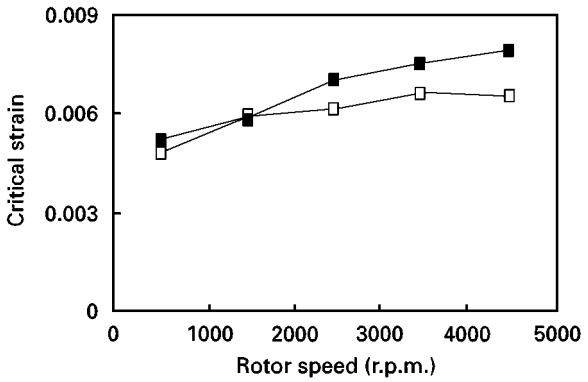

Figure 8 The critical strain, γ_c, as a function of rotor speed of the hammer mill for networks based on (□) unfractionated or (■) fractionated CTMP.

structure) and to a wrinkling of long fibres. Because the fractionated pulp had an almost constant G'_0 in the rotor speed range of 2000–4500 r.p.m., it is plausible that the decrease in G'_0 for the unfractionated pulp is due mainly to the creation of fine material. The very slight decrease in G'_0 of networks based on the fractionated pulp between 2000 and 4500 r.p.m. is probably due to the creation of kinks and curl in the fibres. This is, to some extent, supported by the increase in the curl index in Table I and more strongly by the marked increase in critical strain shown in Fig. 8. The increase in critical strain indicates that each fibre can be deformed to a greater extent before the network yields, i.e. the network can tolerate larger deformations before it starts to deteriorate. This is illustrated in Fig. 9 where the critical strain is shown as a function of the curl index. The fibres straighten before the network yields. (As already mentioned, the network formed by the fibres defibrated at 3500 r.p.m. does not conform with the general pattern in this graph. The corresponding curl index appears to be too low.) The importance of the fibre form for the network properties has also been pointed out by Page *et al.* [6] and by Mohlin and Alfredsson [7].

These conclusions are also supported by the results shown in Fig. 10 which illustrates the effect of the fibre length on the storage modulus and on the critical strain for networks based on the well-defibrated

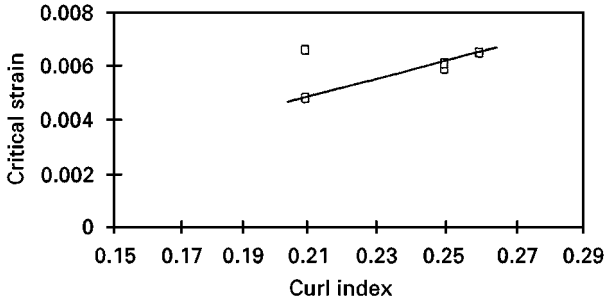

Figure 9 The critical strain of the network as a function of the curl index for unfractionated CTMP.

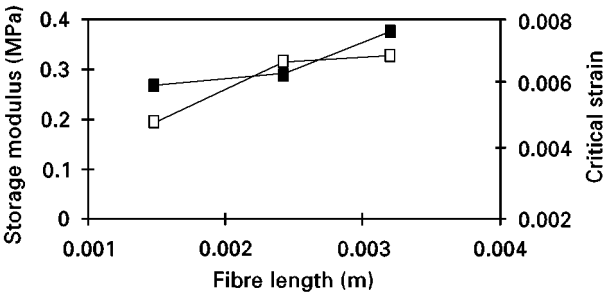

Figure 10 The (□) G'_0 and (■) γ_c plotted against the average fibre length for well-defibrated and fractionated CTMP.

CTMP (i.e. the pulp was defibrated to maximum network strength and then fractionated). Obviously the long-fibre fraction produced a network with a high storage modulus and high critical strain. This is because long fibres, with a large number of contacts per fibre, produce networks which can transfer stress efficiently throughout the structure. Earlier results [3] indicated that an increase in fibre length resulted in a lower storage modulus. This may hold true for networks with different initial densities, i.e. prior to compressing the networks to the same density in the Bohlin rheometer, but it is obviously not the case for networks of CTMP with almost the same initial density. The results for the critical strain are, however, in accordance with the results presented earlier [3]; longer fibres resulted in a higher critical strain.

3.2. Influence of the type of fluff pulps on G'_0 and γ_c

Because most of the fluff pulps produced today are bleached chemical pulps, it was of interest to compare the CTMP with two chemical pulps of different geographical origins. The influence of the different types of fibres on the mechanical properties of the networks was thus investigated. The networks based on the three fluff pulps were also compared with networks of rayon fibres. Two types of homogeneous rayon fibres were used; one had a fibre weight of 100 $\mu g\ m^{-1}$ (diameter 13 μm) and the other a fibre weight of 500 $\mu g\ m^{-1}$ (diameter 30 μm). The pulp fibres used were substantially more inhomogeneous than the rayon fibres and had fibre weights in the range of 170–400 $\mu g\ m^{-1}$. For networks based on rayon fibres,

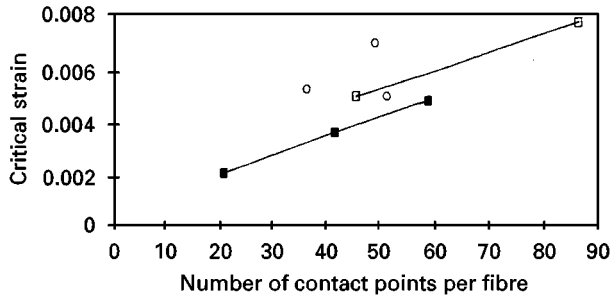

Figure 11 The critical strain versus the number of contact points per fibre in networks based on different fluff pulps and rayon fibres: (□) rayon 100 μg m^{-1}, (■) rayon 500 μg m^{-1}, (○) fluff pulps.

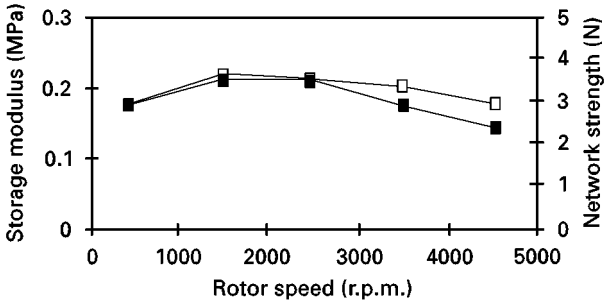

Figure 12 (□) Storage modulus and (■) network strength of the network based on CTMP as a function of rotor speed (defibration energy).

it was noted [3] that there was a fairly good correlation between the critical strain, γ_c, and the number of contact points per fibre, n_f, in the network. This is shown in Fig. 11, where the number of contact points per fibre is evaluated from $n_f = l/S$ where l is the fibre length and S is the free fibre segment length. The corresponding results for the pulp fibres are also included in this graph and they conform approximately to the general pattern observed. The apparent scatter noted for the networks based on the pulp fibres is probably due to differences in fibre shape and fibre flexibility, as well as surface morphology which may affect the strain level at which the network starts to deteriorate.

It was not, however, possible to find a structural parameter (relating to the network) that could be correlated with G_0' when the networks were based on different fibres. This may not be surprising, because G_0' can be expected to depend quite markedly on the fibre stiffness and this is likely to differ for the fibre systems used here.

3.3. Comparison of applied methods – different defibrated CTMP

In order to compare the results obtained with the rheometer and the end-use properties of the networks, a mechanical evaluation was also conducted with the specially designed equipment where networks could be tested in the shear mode. A standard type of strength testing [4] was also performed. Fig. 12 shows the storage modulus and the strength of the CTMP networks as a function of the rotor speed. The two curves appear to be related to the rotor speed in approximately the same way. The influence of the rotor speed on storage modulus and maximum shear force is shown in Fig. 13. The maximum shear force also depended on the rotor speed (defibration energy) in a manner resembling that of the storage modulus. Obviously all the three mechanical measures are related. A network with a low network strength or a low maximum shear force also exhibited a low storage modulus, and vice versa. The critical strain, γ_c, and γ_{max} from the shear testing were also related, i.e. when the γ_{max} increased, the critical strain also increased.

The mechanical properties of the networks can also be described by the elastic energy given by Equation 1,

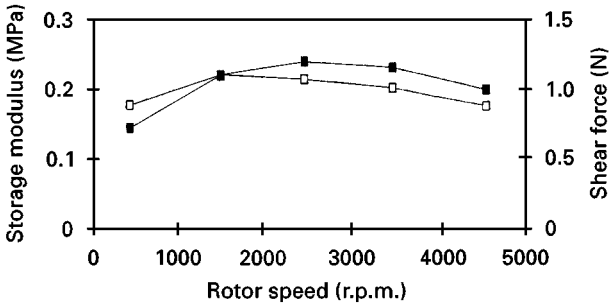

Figure 13 (□) Storage modulus and (■) maximum shear force of the network based on CTMP as a function of rotor speed (defibration energy).

and the work of deformation at rupture as measured in the shear tester. These quantities indicate the energy required to induce yielding and rupture, respectively, of the networks. The elastic energy and the work of deformation at rupture were strongly related, i.e. networks with high elastic energy also showed high work of deformation at rupture.

4. Discussion

The results obtained with the dynamic-mechanical instrument, Bohlin VOR Rheometer, and the shear tester, are obviously related. The two methods probably provide information about the same process but not on the same structural level. First there is a straightening of curved fibre segments and then a disentanglement of fibres in the network as the imposed deformation increases. The fibres do not, however, break. The process can schematically be depicted as follows: in the unstrained network the segments curve, Fig. 14a, then at a small deformation the segments straighten, Fig. 14b, but the contact points between the fibres remain fixed with regard to the fibre surface, i.e. there is no slippage between different fibres. The modulus of the network is more or less unaffected by the deformation, as revealed by the measurements with the rheometer below γ_c. When the network is subjected to higher deformations, the fibre contact points begin to slip and the free segment length between the contact points increases, Fig. 14c. In this region, the storage modulus, G', decreases as a result of the deterioration of the network. Finally, at high deformations, the fibres disentangle and the

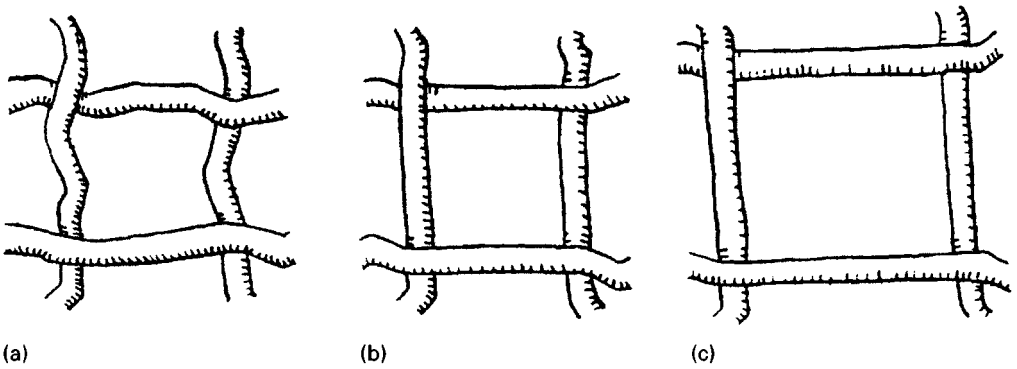

Figure 14 Schematic straining of fibre segments in the network.

network ruptures. This occurs in the shear tester but not in the rheometer.

The similarity between the results obtained in the Bohlin equipment and in the shear tester can be further illustrated by comparison of the corresponding stress–strain curves (or load–deformation behaviour). In the case of the dynamic-mechanical measurements, the stress is obtained from the product of $G'(\gamma)$ and γ. The corresponding stress–strain curves for CTMP networks based on fibres defibrated at different rotor speeds are shown in Fig. 15. The curves are clearly curvilinear, as are the load–deformation curves from the shear tester, at deformations higher than γ_c. Furthermore, the curves fall in the same sequence for both methods. As discussed earlier, the differences due to the choice of rotor speed between the stress–strain curves in Fig. 15 can be explained in terms of differences in fibre curl, content of fines, etc.

The stress–strain curve constructed from the dynamic-mechanical analysis thus corresponds to the initial part of the load–deformation curve obtained with the shear tester and, characterizes the initial (linear) straining of the network and the initial disentanglement of the network. The shear tester provides data relating to the disentanglement process (but not when the network starts to yield) and to the ultimate behaviour of the network.

The effect of the defibration energy on the network structure and on its mechanical properties depends on whether or not the rotor speed chosen is sufficient to produce the maximum network strength. At lower rotor speeds, an increase in the defibration energy (rotor speed) may increase the number of free fibres per unit volume and the number of contact points in the network. This will result in: (i) a shorter free segment length, with the consequence that G'_0 and F_{max} increase; and (ii) a higher number of fibre-to-fibre contact points, with the consequence that the critical strain, γ_c, and the maximum strain, γ_{max}, increase.

At rotor speeds higher than that required to reach the maximum network strength, the defibration is in a sense too powerful, with the result that an increase in the rotor speed leads to a cutting of long and free fibres and also a change in the fibre shape. This results in: (i) a higher content of fine material and fewer long fibres which can transfer stress throughout the network, with the consequence the G'_0 and F_{max} decrease; and (ii) a higher curl index, with the consequence that the critical strain, γ_c, and the maximum strain, γ_{max}, increase.

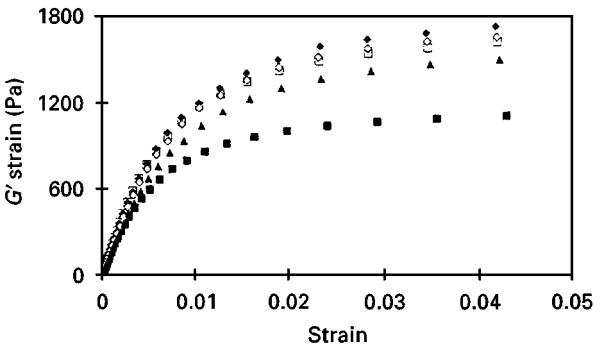

Figure 15 Stress–strain curves for networks based on CTMP defibrated at different rotor speeds. The curves were constructed from the dynamic-mechanical results obtained with the rheometer. (■) 500 r.p.m., (□) 1500 r.p.m., (◆) 2500 r.p.m., (◇) 3500 r.p.m., (▲) 4500 r.p.m.

Thus, from a mechanical point of view, the ideal dry-defibration process should provide a larger number of free fibres per unit volume without producing fine material, at the same time as the curl index should increase. Long and curled fibres are then to be preferred. Information about this kind of results has not been found in the literature.

In this study, it was found that changes in the defibration conditions affected G'_0 (rheological measurements) and F_{max} (from the shear tester) in the same manner. This relation between G'_0 and F_{max} does not, however, necessarily have to hold in all situations, e.g. when the surface characteristics of the fibres are altered. This will be discussed in a forthcoming paper.

5. Conclusions

The most important results of this study can be summarized as follows.

1. The two methods utilizing the dynamic-mechanical instrument (Bohlin VOR Rheometer) or the shear tester, provide information regarding the breakdown of dry-formed fibre networks, but on a different structural level.

2. The defibration process affected the storage shear modulus, G'_0, and the maximum force, F_{max}, in the same manner.

3. If the deformability of the cellulosic network before rupturing is to be improved, long and curled fibres are to be preferred. The networks should exhibit high values of the storage modulus, G'_0, the maximum force, F_{max}, the critical strain, γ_c, and the maximum strain, γ_{max}.

4. The ideal dry-defibration process should provide a larger number of free fibres per unit volume without producing fine material, at the same time as the curl index should increase.

5. Networks based on different fluff pulps can be characterized by the critical strain, γ_c, which in turn depends on the number of contact points per fibre, n_f, in the network, when the network starts to deteriorate.

Acknowledgements

The authors thank the Swedish National Board for Industrial and Technical Development and SCA Research for financial support. SCA and Mölnlycke are also thanked for allowing the publication of the results. Dr J. A. Bristow is thanked for the linguistic revision. Many thanks are also extended to Ms Carin Bergström and Ms Maria Johansson for help with the experimental work.

References

1. T. JOUSIMAA, *Paper Technol. Ind.* **29**(1) (1988) 14.
2. *Idem*, in "2nd International Conference on Nonwovens – absorbency", Vol. **1**, paper (7), (1989), Denmark.
3. C. ASKLING, L. WÅGBERG and M. RIGDAHL, Rheological characterization of dry-formed networks of rayon fibres, 1995, to be published.
4. PFI-Method of 1981, "Measurement of network strength in dry fluffed pulps", (The Norwegian Pulp and Paper Research Institute, Box 250, Vinderen, Oslo 3, Norway, 1981).
5. STFI, Swedish Pulp and Paper Research Institute, Box 5604, 11486 Stockholm, Sweden, Contact Håkan Karlsson.
6. D. H. PAGE, R. S. SETH, B. D. JORDAN and M. C. BARBE, in "8th Fundamental Research Symposium", 1981, Vol. 1, edited by V. Punton, (Mechanical Engineering, London) pp. 183–227.
7. U.-B. MOHLIN and C. ALFREDSSON, in "EUCEPA 24th Conference Proceedings", (Pulp Technology and Energy, Stockholm, 1990) pp. 207–21.

Received 6 March
and accepted 5 December 1997